LANGMUIR Article
Cite This: Langmuir XXXX, XXX, XXX−XXX
pubs.acs.org/Langmuir

Surface-Initiated Poly(oligo(2-alkyl-2-oxazoline)methacrylate) Brushes

Pei Tang,[†,‡] Stefania di Cio,[†,‡] Wen Wang,[†,‡] and Julien E. Gautrot*[,†,‡]

[†]Institute of Bioengineering and [‡]School of Engineering and Materials Science, Queen Mary, University of London, Mile End Road, London E1 4NS, U.K.

Supporting Information

ABSTRACT: Polymer brushes are particularly performant antifouling coatings, owing to their high grafting density that prevents unwanted biomacromolecules to diffuse through the coating and adhere to the underlying substrate. In addition to this structural feature, polymer brushes require a relatively high level of hydrophilicity and a globally neutral structure to display ultrahigh protein resistance. Poly(2-alkyl-2-oxaolines) are attractive building blocks for such coatings as they can display relatively high hydrophilicity, owing to their amide repeat units, but can also be side-chain and end-chain functionalized relatively readily. However, poly(2-alkyl-2-oxazolines) have not yet been introduced through a radical-mediated grafting from polymer brush structure that would confer the high level of grafting density that is the hallmark of highly protein resistant brushes. Here, we present the formation of a series of poly(oligo(2-alkyl-2-oxazoline)methacrylate) brushes generated via a grafting from approach, via atom transfer radical polymerization. We characterize the chemical structure of the resulting coatings via ellipsometry, Fourier-transform infrared spectroscopy, and X-ray photoelectron spectroscopy. We show that allyl end groups can be introduced as a side chain of these brushes to allow functionalization via thiol-ene chemistry. We demonstrate the excellent protein resistance of these coatings in single protein solutions as well as serum solutions at concentration typically used for cell culture. Finally, we demonstrate the feasibility of using these brushes for the micropatterning of cells and the generation of cell-based assays.

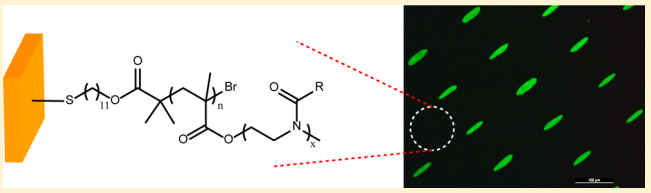

1. INTRODUCTION

Polymer brushes such as those based on poly(oligo(ethylene glycol)methacrylate) (POEGMA), sulfobetaine methacrylate (PSBMA), carboxybetaine methacrylate (PCBMA), and hydroxypropyl methacrylamide (PHPMAm) display exceptional antifouling properties that remain unmatched by other coatings developed to date.[1−6] In particular, PCBMA and PHPMAm and parent brushes display zero fouling levels upon exposure to plasma and serum,[2,4,7] making these coatings particularly attractive for biosensing applications. While POEGMA is perhaps slightly less protein-resistant,[2,8] it has the advantage of being relatively cheap and readily available. Although the protein resistance of these brushes is not fully understood at a molecular level, it was proposed to result from the combination of their high hydration and the extremely dense packing and crowding that can be achieved via surface-initiated polymerization.[9−12] In this respect, surface-initiated polymer brushes perform significantly better than those grafted to substrates, postpolymerization.[7,8]

Despite these exceptional properties, the biofunctionalization of polymer brushes for the design of a polymer brush-based platform for biomedical applications remains challenging (i.e., biosensing, tissue engineering, cell-based assays, and targeted drug and gene delivery).[5,13,14] This is partially due to the lack of infiltration of protein or even peptides within antifouling polymer brushes, requiring particularly efficient coupling strategies.[15−17] In addition, strategies developed to date for the side-chain biofunctionalization of polymer brushes such as POEGMA or PCBAAm typically require brush activation prior to coupling. It is therefore important to develop new generations of polymer brushes that would allow more direct biofunctionalization while retaining excellent control of brush structure and antifouling properties.

Poly(2-alkyl-2-oxazolines) (POx) are attractive candidates for such applications as they display antifouling properties that compare favorably to poly(ethylene glycol) (PEG) derivatives[18−21] because of their ability to sustain the formation of hydrogen-bonded water networks and associated level of hydration.[22] POx have been applied to the design of bioconjugates and drug delivery systems and the formation of hydrogels that display controlled cell adhesion, similar to PEG-based systems.[19,23,24] Typically, POx are generated via the cationic ring opening polymerization of corresponding 2-alkyl-2-oxazolines, often initiated by alkyl-bromides or tosylates.[25−27] These reactions occur in relatively mild conditions under inert atmosphere and tolerate some level of functionalization of the alkyl-side chains as these are relatively remote from the reactive center.[26,28] Hence butenyl and decenyl residues can conveniently be introduced as side chains of POx, for subsequent biofunctionalization or cross-link-

Received: May 22, 2018
Revised: July 19, 2018
Published: July 21, 2018

DOI: 10.1021/acs.langmuir.8b01682
Langmuir XXXX, XXX, XXX−XXX

ing.[29−37] In addition, the reasonable control of POx end chains, determined by the control of initiation from alkylbromides and tosylates and that of termination steps with a range of nucleophiles, allows the rational design of telechelic POx, for example displaying methacrylate groups suitable for further polymerization.[38,39]

A number of strategies have been developed for the use of POx as surface coatings, to confer hydrophilicity and antifouling properties to corresponding substrates.[40] POx coatings have been developed via cationic ring opening polymerization of oxazoline monomers,[41,42] the grafting of thiol-terminated poly(oligo(oxazline)methacrylate) copolymers to gold substrates,[43] carboxylic acid- and amine-terminated POx to epoxide-coated substrates,[44,45] the adsorption of block- and graft-copolymers of POx and polyelectrolytes,[19,46,47] incorporation as a side chain of poly(urethanes),[48] grafting through of oxazoline side chains in polymer brushes,[49] and the cross-linking of spin-coated POx films.[50] These coatings display comparable protein resistance to PEGs in single protein solutions,[19,43,50] although their performance in more complex solutions (e.g., serum or plasma) has not been studied systematically via surface plasmon resonance (SPR) or quartz crystal microbalance. Recently, "grafted-to" cyclic POx were shown to display improved antifouling properties and lubricity, compared to their linear parents, owing to their denser packing.[51,52] Hence, POx appear as attractive protein-resistant coatings but have not yet been incorporated through a surface-initiated radical polymerization approach.

In this report, we present the grafting of poly(oligo(2-alkyl-2-oxazoline)methacrylates) (POAlkOxMA) via surface-initiated atom transfer radical polymerization (SI-ATRP). We characterize the surface chemistry of the resulting coatings via ellipsometry, infrared spectroscopy, X-ray photoelectron spectroscopy (XPS), and water contact goniometry. We demonstrate the simple functionalization of brushes displaying allyl residues at the terminal position of their side chains, via thiol-ene chemistry, therefore bypassing the need for activation prior to coupling. In addition, we report the excellent protein resistance of POAlkOxMA brushes in albumin, fibronectin, and serum solutions, in comparison to PEG self-assembled monolayers and POEGMA brushes. Finally, we demonstrate the applicability of POAlkOxMA brushes for the design of cell micropattern arrays.

2. EXPERIMENTAL SECTION

2.1. Chemicals and Materials. Methyl *p*-toluenesulfonate (98%), allyl *p*-toluenesulfonate [≥95.0% (GC)], acetonitrile (anhydrous, 99.8%, stored under argon), methacrylic acid (MAA, contains 250 ppm MEHQ as inhibitor, 99%), sodium chloride (99.5%), sodium bicarbonate (99.5%), magnesium sulfite (98%), dithranol [≥90% (HPLC)], chloroform (AR), copper(II) bromide (99.999%), 2,2′-bipyridyl (>99%, bpy), methanol, PEG methyl ether methacrylate (average M_n 300), L-glutathione reduced (98%), 4′,6-diamidino-2-phenylindole (DAPI), phalloidin, chloroform-*d* (>99.8%), 2-ethyl-2-oxazoline (EtOx, 99%), and 2-methyl-2-oxzoline (MeOx, 98%) were purchased from Sigma-Aldrich. EtOx and MeOx monomers were dried over calcium hydride and distilled under argon prior to use. Triethylamine (≥99.5%) was dried over potassium hydroxide and distilled under argon prior to use.

2.2. Synthesis of Oligo(2-alkyl-2-oxazoline)methacrylates. *2.2.1. Synthesis of Oligo(2-ethyl-2-oxaoline)methacrylate.* Methyl tosylate (0.188 g, 1.01 mmol), 2-ethyl-2-oxaoline (0.500 g, 5.04 mmol), and acetonitrile (7.0 mL) were added in a dried microwave vial. The vial was sealed with a dedicated vessel cap and placed in a microwave synthesizer. The reaction solution was heated to the desired temperature (140 °C) after around 20 s preheating and kept at this temperature while stirring for the desired reaction time (5−30 min). Subsequently, reaction mixtures were cooled to room temperature under a gas flow. Triethylamine (0.408 g, 4.03 mmol) was added in a 4-fold excess, followed by MAA (0.024 g, 3.02 mmol) in a 3-fold excess, via a syringe, through the microwave vessel cap. The reaction solution was heated to 80 °C for 12 h. Acetonitrile was evaporated and the polymer was dissolved in chloroform. The solution was washed three times with saturated sodium bicarbonate aqueous solution and then washed with brine three times. Finally, the solution was dried with magnesium sulfate and filtered, before the solvent was evaporated under reduced pressure, and the resulting yellow liquid polymer was dried under high vacuum and stored in a fridge. ^{1}H NMR (400 MHZ, $CDCl_3$, see Figure 1 for spectrum): δ 6.07 (=CH_2), 5.58 (=CH_2), 4.27 (m, CH_2−OCO), 3.44 (m, N−CH_2), 3.02 (m, N−CH_3), 2.35 (m, CO−CH_2−C), 1.92 (m, CH_2=C−CH_3), 1.12 (m, C−CH_3).

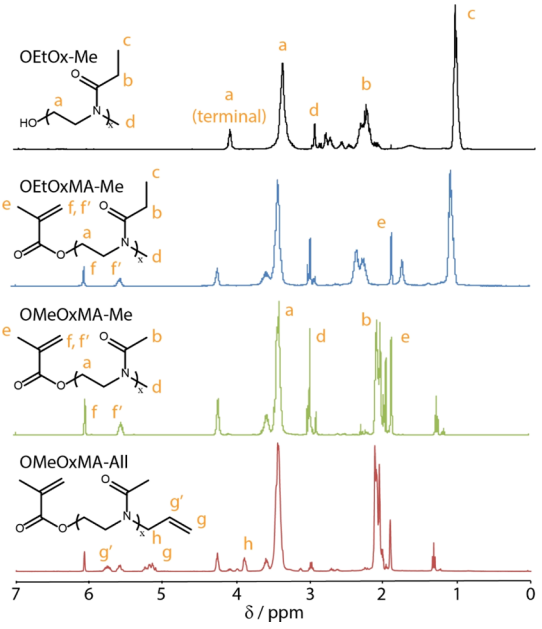

Figure 1. ^{1}H NMR spectrum in $CDCl_3$ of oligo(2-alkyl-2-oxazolines) initiated with methyl tosylate or allyl tosylate and terminated by reaction with water or MAA.

2.2.2. Synthesis of Oligo(2-methyl-2-oxaoline)methacrylate. This was synthesized as above, from methyl tosylate (0.219 g, 1.18 mmol), 2-methyl-2-oxaoline (0.500 g, 5.88 mmol), acetonitrile (2.0 mL), triethylamine (0.477 g, 4.71 mmol), and MAA (0.028 g, 3.53 mmol). ^{1}H NMR (400 MHZ, $CDCl_3$, see Figure 1 for spectrum): δ 6.05 (=CH_2), 5.56 (=CH_2), 4.24 (m, CH_2−OCO), 3.42 (m, N−CH_2), 3.00 (m, N−CH_3), 2.09 (m, CO−CH_3 and CH_2=C−CH_3).

2.2.3. Synthesis of Oligo(2-methyl-2-oxaoline)methacrylate, Allyl Tosylate Initiated. This was synthesized as above, from allyl tosylate (0.249 g, 1.18 mmol), 2-methyl-2-oxaoline (0.500 g, 5.88 mmol), acetonitrile (2.0 mL), triethylamine (0.477 g, 4.71 mmol), and MAA (0.028 g, 3.53 mmol). ^{1}H NMR (400 MHZ, $CDCl_3$, see Figure 1 for spectrum): δ 6.07 (=CH_2), 5.77 (m, CH_2=CH−CH_3), 5.59 (=CH_2), 5.15 (=CH_2), 4.27 (m, CH_2−OCO), 3.44 (m, N−CH_2), 2.09 (m, CO−CH_3 and CH_2=C−CH_3).

2.3. Generation of Polymer Brushes via Surface-Initiated ATRP. For the growth of a 20 nm-thick POEtOxMA-Me brush: a solution of $CuBr_2$ (18 mg, 80 μmol) and bpy (320 mg, 2.0 mmol) in water/methanol 2/1 (15 mL) was degassed using nitrogen bubbling for 30 min. CuBr (82 mg, 0.57 mmol) was added to this solution and the resulting mixture further degassed for 10 min, to make solution A. A solution of POEtOxMA-Me (4.2 g, 7.2 mmol) in water/methanol

DOI: 10.1021/acs.langmuir.8b01682
Langmuir XXXX, XXX, XXX−XXX

2:1 (5 mL) was degassed using nitrogen bubbling for 30 min. Solution A (5 mL) was transferred to the monomer solution, stirred for 1 min, and then transferred to degassed tubes containing the initiator-coated gold substrates (generated by immersion in 25 mL ethanol solutions of 39 mg thiol initiator overnight) under an inert atmosphere. The polymerization was stopped after the desired reaction time (up to 360 min) by immersing the surface in deionized water and subsequently washed with a large amount of water and ethanol before drying in a stream of nitrogen. POMeOxMA-All brushes and POMeOxMA-Me brushes were grown following this protocol, stopping polymerizations at 240 and 360 min, for 6 and 12 nm brushes, respectively.

2.4. Thiol-ene Functionalization of Polymer Brushes. A photoinitiator solution (25 μL; Irgacure 2959 with concentration of 250 mg/mL in methanol) was added to 1 mL of glutathione solution [14 mg/mL in phosphate-buffered saline (PBS)]. The resulting solution (10 μL) was deposited on a quartz plate and polymer brush-functionalized gold substrates were placed on top, face down. Substrates were exposed to UV radiation for 300 s (intensity: 17 mW/cm^2) and washed with deionized water before measurement of their thickness by ellipsometry or further surface analysis. Functionalization levels were quantified from ellipsometric thicknesses before and after thiol-ene coupling using the following equation:

$$f_1 = \frac{\Delta h_d M_0}{h_{d_0} M_x} \times 100 \quad (1)$$

where f_1 is the functionalization level (in %), Δh_d is the change in dry ellipsometric thickness, h_{d_0} is the starting ellipsometric thickness, M_o is the molar mass of the pristine polymer brush repeat units, and M_x is the molar mass of the fragment added via thiol-ene coupling.

2.5. Cell Micropatterning Using Polymer Brushes. GEβ3 cells[53] were cultured in Dulbecco's modified Eagle's medium (DMEM) supplemented with 10% fetal bovine serum (FBS), glutamine, and antibiotics. Cells were cultured to confluency (about 80% densities) and were detached using trypsin/versene (1:9) and reseeded on the samples in a 48 well plate at a density of 7500 cells/well (0.5 mL/well) in DMEM medium. Cells were then allowed to adhere for 24 h and then fixed and immunostained. After 24 h incubation, the cells were fixed with 4% paraformaldehyde (in PBS) for 10 min, permeabilized with 0.2% Triton X-100 (in PBS) for 5 min, and blocked with a solution of 10% FBS and 0.25% gelatin for 1 h at room temperature. Phalloidin (for actin staining, 1:500) was added at this stage too. The samples were then incubated in DAPI (for nuclear staining, 1:1000) for 1 h at room temperature and washed again before mounting on glass slides with Mowiol solution.

2.6. Characterization of Polymers and Surfaces. ^{1}H NMR characterization was carried out using Bruker AV 400 and AVIII 400. Abbreviations for NMR peaks: s-singlet, d-doublet, t-triplet, and m-multiplet. For end chain analysis, the initiator to end chain ratios were calculated as follows: the peak integrations were first divided by the number of corresponding protons, and ratios were based on H_i (corresponding to methyl initiators), H_m (corresponding to polymerized repeat units), and H_t (corresponding to methacrylate end chains). Dry brush thicknesses were measured by ellipsometry at a 70° incidence angle using an α-SE instrument from J.A. Woolam co. Inc. A simple gold substrate/Cauchy film model was used and fitted between 400 and 900 nm. Grazing angle FTIR was produced by a Bruker Tensor 27 spectrometer equipped with an MCT detector; results were acquired with a total of 128 scans per run in the region of 400−4000 cm^{-1}. The UV light that was used to carry and initiate thiol-ene reactions was generated with an OmniCure series 1500 lamp. The radiometer that was used to measure the UV intensity was from International light technologies, ILT 1400-A radiometer photometer. A Leica DMI4000B epifluorescence microscope fitted with an HCX PL FLUOTAR (20 × 0.7 NA lens, 63 × 1.40 Oil lens) PJ1 objective, and a Leica DFC300 FX CCD camera was used to image patterned surfaces. Image J was used for analysis of epifluorescence microscopy images. SPR was performed on a Biacore 3000. SPR chips (Ssens) were coated with the desired polymer brush (thicknesses reported in the corresponding figure). Treated chips were docked, primed with buffer (PBS) twice and equilibrated at 20 μL/min for 30 min or until a stable baseline was obtained. For measurements of nonspecific binding, an example of the programmed sequence was as follows: wash with PBS, equilibrate for 5 min, and expose to a protein solution for 5 min (bovine serum albumin (BSA) of 1, 10 μg/mL FN or 10% FBS). The flow rate was 20 μL/min. Measurements were carried out in triplicate.

3. RESULTS AND DISCUSSION

3.1. Synthesis of Oligo(2-alkyl-2-oxazoline)-methacrylates. Oligo(2-alkyl-2-oxazoline)methacrylates were prepared by ring opening polymerization of the corresponding 2-alkyl-2-oxazolines, initiated by alkyl tosylates, in acetonitrile, using a microwave synthesizer. This protocol was previously found to afford a good control of polymer chain growth for 2-ethyl- and 2-methyl-2-oxazolines, enabling end-chain termination with defined moieties.[38,54] Indeed, we obtained oligomers in relatively high yields (86−95%, after purification via extraction). We used methyl tosylate and allyl tosylate as initiators, to afford unreactive methyl and thiol-ene reactive allyl end chains, respectively. Termination was carried out by introducing MAA and trimethylamine at 80 °C, following protocols previously reported.[38] ^{1}H NMR confirmed the structure of the oligomers obtained, with all methacrylates displaying the expected olefinic protons at 5.58 and 6.07 ppm (Figure 1). Only OMeOxMA-All displayed an additional set of olefinic protons at 5.15 and 5.77 ppm, corresponding to the allyl function. End chain analysis (comparing methyl and allyl peaks at 3.02 and 5.15 ppm, for initiators, to olefinic and ester peaks at 4.26 ppm, for terminating agents) confirmed the excellent control of the molecular structures obtained (0.92−1.16, Table 1). This is in good agreement with results obtained for similar oligomers.[38]

Table 1. Summary of End Chain Analysis by NMR and Yields for the Three Methacrylate Terminated Oligomers Synthesized

	M/I	H_m/H_i	H_m/H_t	H_i/H_t	yield (%)
OMeOxMA-All	5/1	4.38	5.08	1.16	86
OMeOxMA-Me	5/1	5.23	4.80	0.92	89
OEtOxMA-Me	5/1	5.63	5.18	0.92	95

The targeted degrees of polymerization were kept relatively low (5 repeat units) to improve the polymerizability of the resulting methacrylate via SI-ATRP. Indeed, previous work highlighted that longer oligo(ethylene glycol)methacrylates display reduced polymerization rates when initiated from surfaces. Whereas SI-ATRP of OEGMA with 5−6 repeat units can be pushed relatively easily to 100 nm and above, longer oligo(ethylene glycol) chains polymerized more slowly.[13,55] This is presumably due to the high steric hindrance that restrict polymerizability, especially in surface-confined reactions. The obtained degrees of polymerizations were in very good agreement with the expected number of repeat units. Hence, our data confirm the preparation of oxazoline oligomers with 5 repeat units and good end group fidelity.

3.2. Surface-Initiated ATRP of Oligo(2-alkyl-2-oxazoline)methacrylates. We next investigated the surface-initiated ATRP of oligo(2-alkyl-2-oxazoline)methacrylates from gold-coated silicon substrates functionalized with bromoisobutyrate initiators (Scheme 1). The grafting density of polymer brushes typically achieved on such systems (whether on gold or silicon substrates functionalized with

DOI: 10.1021/acs.langmuir.8b01682
Langmuir XXXX, XXX, XXX−XXX

Scheme 1. Deposition of ATRP Initiator Onto Gold Substrates and Subsequent ATRP of Oligo(2-alkyl-2-oxazoline)methacrylates

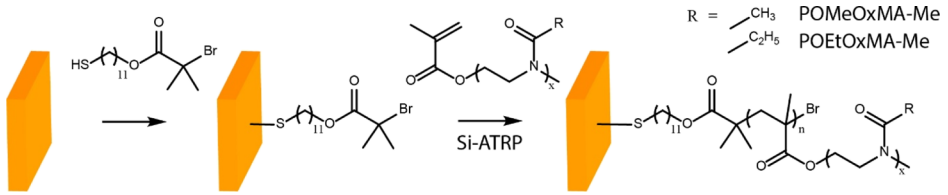

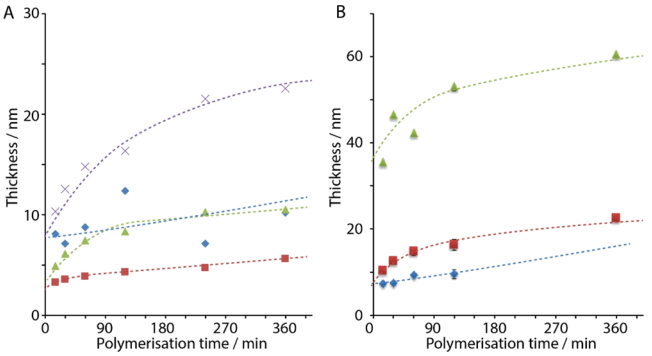

Figure 2. Polymerization kinetics of oligo(2-alkyl-2-oxazoline)-methacrylates characterized via ellipsometry. (A) Polymerization kinetics of POEtOxMA-Me brushes in different catalytic conditions. Blue: water/ethanol (2/1), $CuBr_2$ (18 mg), CuBr (119.65 mg), bipyridine (320 mg); red: water/methanol (4/1), $CuBr_2$ (18 mg), CuCl (82 mg), bipyridine (320 mg); green: water/methanol (2/1), $CuBr_2$ (18 mg), CuCl (82 mg), bipyridine (320 mg); purple: water/methanol (2/1), $CuBr_2$ (18 mg), CuBr (119.65 mg), bipyridine (320 mg). (B) Polymerization kinetics of different types of oligo(2-alkyl-2-oxazoline)methacrylates and oligo(ethylene glycol)methacrylate in identical catalytic conditions (water/methanol (2/1), $CuBr_2$ (18 mg), CuBr (119.65 mg), bipyridine (320 mg)). Blue: OMeOxMA-Me; red: OEtOxMA-Me; green: OEGMA-Me. Dotted lines are only intended as guides for the eye.

monolayers of bromoisobutyrate initiators) is near 0.5 chains/nm^2,[56] corresponding to relatively high packing densities not typically achievable via grafting from approaches. We first examined the impact of solvent composition and catalyst on the kinetics of brush growth (quantified by ellipsometry on dry films, Figure 2). For a 2/1 water/ethanol mixture with CuBr catalyst (composition similar to those used for the growth of POEGMA brushes[13,55]), relatively thin brushes (approximately 10 nm) were obtained, in stark contrast to the brush height obtained in similar conditions for POEGMA.[13,55] Replacing CuBr by CuCl had only a minor impact on brush growth, unlike its effect in other systems.[57] Changing the composition of the solvent had a relatively strong impact on the growth of POEtOxMA-Me (Figure 2), similarly to what has been previously reported for POEGMA.[55,58] At higher aqueous ratios with ethanol, demixion was observed and polymerizations were not attempted. When ethanol was replaced by methanol, demixion was prevented, but the dry ellipsometric thickness of the resulting brushes was below 10 nm, with very little evidence for any control of the brush growth.

The polymerization of three methacrylates was compared next. OEGMA, OEtOxMA-Me, and OMeOxMA-Me were polymerized in identical conditions (solvent composition, catalyst, and monomer concentration), and the evolution of the dry thickness of the resulting brushes was quantified by ellipsometry (Figure 2B). POEGMA growth reached 30 nm

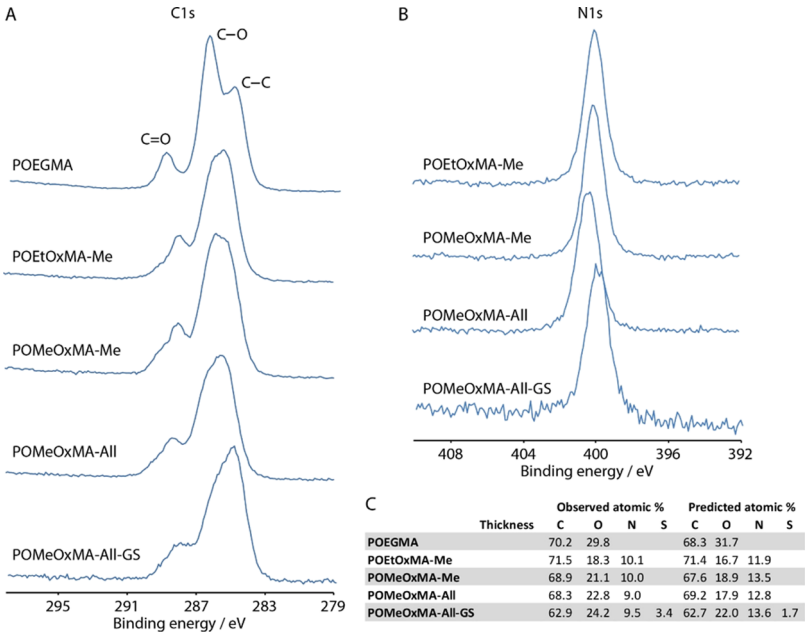

C

	Thickness	Observed atomic % C	O	N	S	Predicted atomic % C	O	N	S
POEGMA		70.2	29.8			68.3	31.7		
POEtOxMA-Me		71.5	18.3	10.1		71.4	16.7	11.9	
POMeOxMA-Me		68.9	21.1	10.0		67.6	18.9	13.5	
POMeOxMA-All		68.3	22.8	9.0		69.2	17.9	12.8	
POMeOxMA-All-GS		62.9	24.2	9.5	3.4	62.7	22.0	13.6	1.7

Figure 3. X-ray photoelectron spectra of poly(oligo(2-alkyl-2-oxazoline)methacrylate) brushes. The thickness of polymer brushes were POEGMA, 13 nm; POEtOxMA-Me, 12 nm; POMeOxMA-Me, 12 nm; POMeOxMA-All, 7 nm; and POMeOxMA-All-GS, 9.5 nm. (A) C 1s spectra. (B) N 1s spectra. (C) Table summarizing corresponding atom compositions.

DOI: 10.1021/acs.langmuir.8b01682
Langmuir XXXX, XXX, XXX−XXX

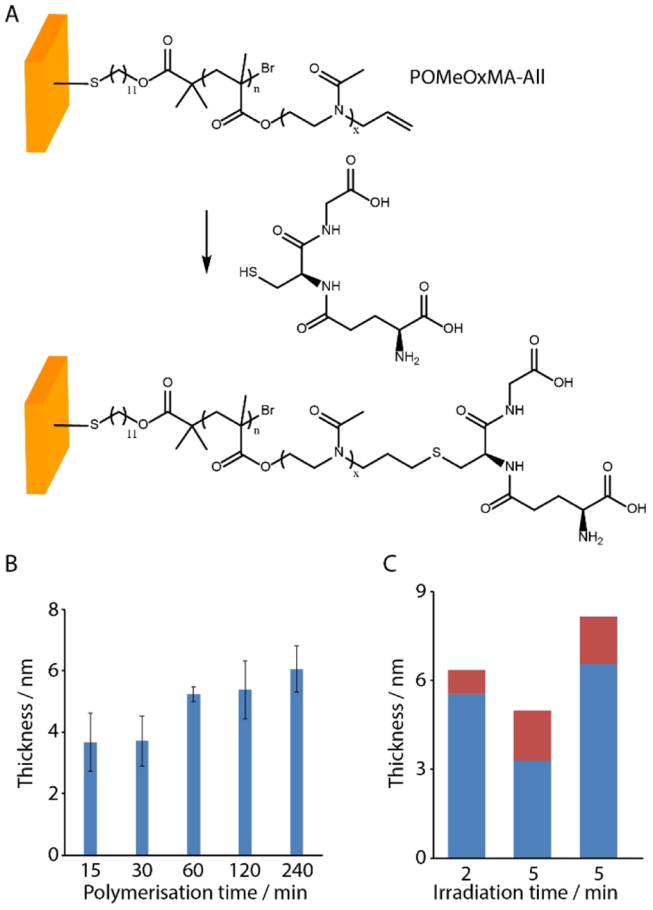

Figure 4. Functionalization of POMeOxMA-All brushes with glutathione via thiol-ene reaction. (A) Scheme representing the functionalization of POMeOxMA-All grown from gold substrates via thiol-ene chemistry. (B) Growth of POMeOxMA-All brushes over 4 h, characterized via ellipsometry. (C) Thickness of POMeOxMA-All brushes before and after reaction with glutathione under different conditions (UV intensity: 17 mW/cm^2, time varied between 2 and 5 min), monitored via ellipsometry.

after 20 min polymerization and continued increasing at a slower pace thereafter, reaching 60 nm after 6 h of polymerization. Although this indicates a lack of full control of the polymer brush growth, this is in good agreement with previous reports that highlighted an initial burst of polymerization for POEGMA brushes, especially with fast initiating systems such as those based on bipyridine.[55] Similarly, POEtOxMA-Me and POMeOxMA-Me displayed an initial burst, although weaker (10 nm), followed by a more gradual increase in brush thickness. This allowed POEtOxMA-Me brushes with thicknesses of 20 nm, while POMeOxMA-Me remained below 15 nm. Overall, the thicknesses achieved were comparable to the thicknesses of other protein resistant brushes previously studied, for which a thickness of 20−30 nm was found to be ideal to reduce nonspecific binding,[3,59,60] but the growth of our POx brushes remained relatively uncontrolled. Although such lack of control has been reported for a wide range of brushes,[4,57,61] future efforts will focus on identifying potential contaminants resulting in this lack of control and catalytic systems helping to promote more sustained brush growth.

The surface chemistry of the brushes synthesized was investigated next, to confirm the control of the structure of the coatings generated. FTIR confirmed the oligo(oxazoline) structure of POEtOxMA-Me and POMeOxMA-Me, with C−H stretching bands near 2950 cm^{-1}, higher than those observed in POEGMA (2920 cm^{-1}), and strong amide bands at 1643 cm^{-1}, in addition to the carbonyl stretching band observed at 1730 cm^{-1} for POEGMA. Similarly, whereas POEGMA brushes display a group of bands with a peak centered at 1142 cm^{-1}, corresponding to C−O−C asymmetric stretching and CH_2 rocking and twisting,[62] C−N stretching and associated CH_2 bands were shifted to 1153 and 1167 cm^{-1} in POEtOxMA-Me and POMeOxMA-Me brushes (Figure S1). XPS provided further confirmation of the structures of these polymer brushes (Figure 3). Whereas POEGMA brushes did not display any nitrogen content, as expected, POEtOxMA-Me and POMeOxMA-Me displayed approximately 10% of nitrogen, as predicted (Figure 3B,C; differences with predictions may arise from partial probing of the underlying silicone oxide layer, resulting in the enrichment in oxygen content). In addition, the C 1s spectra displayed a stronger C−O component (at 286.0 eV) in the case of POEGMA brushes, compared to the C═O and C−C peaks (at 288.6 and 284.6 eV, respectively), in agreement with their oligo(ethylene glycol) structure (Figure 3A; note that this leads to the overlap of C−C and C−O peaks in oxazoline derivatives, with a maximum at 285.3 eV).

3.3. Surface Functionalization via Thiol-ene Coupling. In order to promote direct functionalization of POx brushes, without postpolymerization activation, allyl-terminated oligo(2-methyl-2-oxazoline)methacrylates (OMeOxMA-All) were polymerized via SI-ATRP (Figure 4). Although allyl groups can potentially cross-react in radical polymerization, their reactivity is so low compared to that of methacrylates and acrylates that they do not need protection.[63] The ellipsometric thickness of dry POMeOxMA-All gradually increased up to 6 nm (Figure 4B) but could not be pushed beyond. This lack of control could be indicative of some deactivation of radicals by pendant allyl residues (allyl methacrylate polymers were previously synthesized in bulk solutions[63] rather than from surfaces) or could be the result of impurities remaining in our monomers despite repeated extraction procedures. XPS confirmed the expected composition of the coatings generated, in agreement with the chemical structure of the corresponding oligo(2-alkyl-2-oxazoline)methacrylates (Figures 3 and S2). Although our results indicated a lack of control of the growth process, we decided to test the reactivity of the resulting brushes via thiol-ene chemistry, as reactivity is typically confined to the upper compartment of polymer brushes, and therefore, a few nm of reactive brushes would be sufficient to achieve comparable densities of functionalization to thicker coatings.[15−17]

Thiol-ene coupling was initiated by a photoradical process, using the initiator Irgacure 2959, as previously reported.[17,64,65] Thiol-ene reactions offer attractive features for biofunctionalization, as they promote coupling directly via cysteines from peptides and proteins, in mild conditions and in conventional buffers or even cell culture medium.[64−67] As a model thiol, we used glutathione, owing to its relatively large size and chemical composition, allowing detection via ellipsometry and XPS.[17,65] After thiol-ene reaction of glutathione on POMeOxMA-All for 5 min (Irgacure 2959 and glutathione at 0.25 and 14 mg/mL in PBS, respectively), the dry brush thickness increased by 20−30%, in agreement with the difference in molar mass between glutathione and the OMeOxMA-All. These changes in

DOI: 10.1021/acs.langmuir.8b01682
Langmuir XXXX, XXX, XXX−XXX

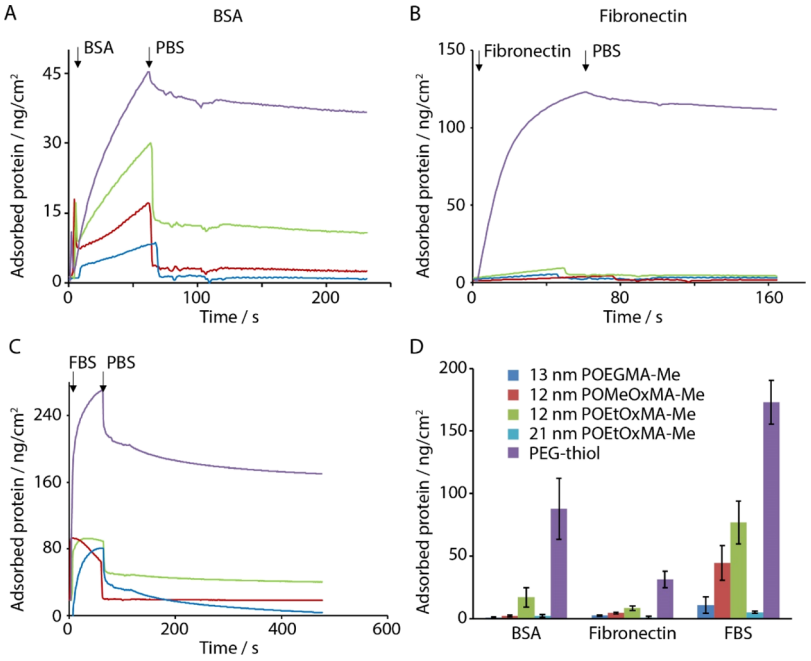

Figure 5. Protein resistance of polymer brushes characterized by SPR. In situ adsorption traces to brushes, from (A) 1 mg/mL BSA solutions, (B) 10 μg/mL fibronectin solution, and (C) 10% FBS solutions. Dark blue, 13 nm POEGMA brushes; red, 12 nm POMeOxMA-Me brushes; green, 12 nm POEtOxMA-Me brushes; purple, PEG thiol monolayers used as control. Arrows indicate the points at which protein solutions were injected and then washed with PBS. (D) Summary of the residual protein adsorption to polymer brushes and control substrates.

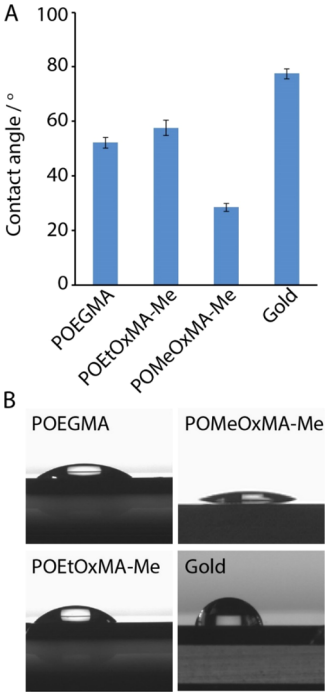

Figure 6. Characterization of the hydrophilicity of polymer brushes via water contact goniometry. (A) Contact angles measured on polymer brushes and gold substrates. The thickness of polymer brushes were POEGMA, 13 nm; POEtOxMA-Me, 12 nm; POMeOxMA-Me, 12 nm. (B) Corresponding representative images.

thickness correspond to functionalization efficiencies ranging from 33 to 77%, depending on the brush thickness and irradiation time (as determined from ellipsometric thicknesses, using eq 1). Such functionalization levels agree well with those reported for allyl-functionalized glycidyl methacrylate brushes with glutathione, in similar conditions.[17] The reduction in functionalization observed for thicker brushes (38% for 7.0 nm instead of 77% for 3.5 nm) is also in good agreement with the known restriction of molecular diffusion through polymer brushes, leading to surface functionalization rather than efficient coupling through the brush.[15,17] Therefore, our results indicate that short blocks of allyl-functionalized brushes should be sufficient to confer relatively high surface functionalization levels. In the absence of initiator or UV irradiation, no change in ellipsometric thickness was observed, confirming the specificity of the coupling. XPS further confirmed the change in the chemistry of the functionalized brush, with a marked decrease in carbon content and an increase in oxygen content, as well as the presence of sulfur, to levels expected from the molecular structure of the resulting brushes (Figure 3). Therefore, thiol-ene functionalization of allyl-substituted oligo(oxazoline)methacrylates appears as a promising methodology for the direct functionalization of polymer brushes.

3.4. Protein Resistance of Poly(oligo(2-alkyl-2-oxazoline)methacrylate Brushes. We next characterized protein adsorption to POx brushes by growing brushes from the surface of SPR chips (through tethering via thiol ATRP initiator monolayers) and exposing the resulting surfaces to solutions of albumin (BSA, a protein particularly abundant in serum), fibronectin (an extracellular matrix (ECM) protein regulating cellular adhesion), and FBS (commonly used for cell culture at 10% concentrations). POEtOxMA-Me (12 and 21 nm) and POMeOxMA-Me (12 nm) brushes were compared to POEGMA brushes (13 nm) and PEG-thiol monolayers (obtained via direct grafting of thiol-terminated PEG with a M_w of 1000 g/mol to the gold-coated SPR chips; Figure 5). All coatings performed significantly better compared to the PEG monolayer. In particular, the 13 nm POEGMA and 21 nm POEtOxMA-Me showed only very little residual adsorption from all protein solutions, in agreement with previous results

DOI: 10.1021/acs.langmuir.8b01682
Langmuir XXXX, XXX, XXX−XXX

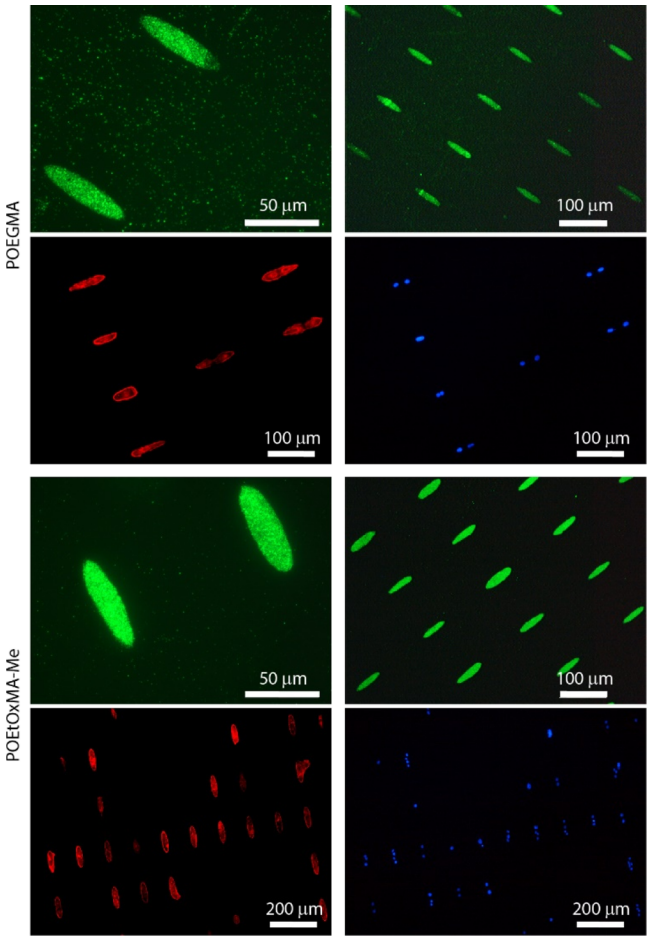

Figure 7. Deposition of fibronectin on patterned POEGMA and POEtOxMA-Me brush substrates. Patterning of fibronectin (top images, green) and fluorescence microscopy images of GEβ3 cells (red, phalloidin; blue, DAPI) spreading on adhesive islands defined by POEGMA and POEtOxMA-Me brushes.

obtained for POEGMA.[6,13,55] When the thickness of POEtOxMA-Me was reduced to 12 nm, protein adsorption increased, in particular for BSA and FBS. This is perhaps due to the slightly increased hydrophobicity of POEtOxMA-Me, compared to POEGMA (Figure 6) and the ease with which albumin denatures and adsorbs at hydrophobic interfaces.[68] When POMeOxMA-Me was used instead, protein adsorption remained low, except for FBS solution for which intermediate values were observed compared to POEGMA and POEtOxMA-Me. Interestingly, protein adsorption, from FBS solutions in particular, did not correlate with the coating hydrophilicity (POMeOxMA-Me displayed by far the more hydrophilic character, Figure 6). This suggested that small molecules from serum were able to diffuse through these thin brushes and adhere onto the underlying substrate. Overall, these results indicate that poly(oligo(2-alkyl-2-oxazoline)-methacrylate brushes display particularly promising protein resistance and should be attractive coatings for the design of biosensors and for cell array formation.

3.5. Cell Patterning with Poly(oligo(2-ethyl-2-oxazoline)methacrylate Brushes. To demonstrate the applicability of poly(oligo(2-alkyl-2-oxazoline)methacrylate brushes in biotechnologies, we micropatterned POEGMA and POEtOxMA-Me brushes via microcontact printing of a thiol-terminated ATRP initiator.[58,69,70] After brush growth, this allows the direct deposition of ECM proteins that promote cell adhesion to defined areas determined by the patterned brush geometry. The quality of the ECM patterns generated (after fibronectin deposition) was characterized first by immunostaining (Figure 7), indicating clear elliptical areas, as expected from the original dimensions of the PDMS stamps used for microcontact printing (7850 μm^2). A slightly cleaner background was observed for POEtOxMA-Me patterns, perhaps reflecting the slightly improved protein resistance of this coating at 20 nm thicknesses (Figure 5). In turn, cells adhered and spread well on both POEGMA and POEtOxMA-Me micropatterns, displaying elongated shapes and a structured actin cytoskeleton polarized in the main axis of the adhesive islands.[71] No apparent cell adhesion to the brush background was observed, consistent with the protein resistance observed for these coatings. Overall, our results indicate that poly(oligo(2-alkyl-2-oxazoline)methacrylate brushes are promising candidates for the design of cellular microarrays for cell-based assays such as shape-induced differentiation.[71,72]

4. CONCLUSIONS

Our results indicate that poly(oligo(2-alkyl-2-oxaoline)-methacrylates) are promising candidates for the design of protein-resistant polymer brushes. The synthesis of the corresponding macromonomers is relatively straightforward and scalable but could be further improved to better control the polymerizability of corresponding brushes. This is in particular important for allyl-functionalized monomers, in addition to the protection of the allyl group. However, such allyl or other alkene derivatives are attractive candidates for the direct functionalization of polymer brushes via thiol-ene coupling, without postpolymerization activation. Furthermore, we reported the excellent protein resistance of poly(oligo(2-alkyl-2-oxazoline)methacrylate) brushes, even in the presence of serum solutions, and demonstrated the proof-of-concept of their use for the design of protein micropatterns for cell-based assays.

■ ASSOCIATED CONTENT

Supporting Information

The Supporting Information is available free of charge on the ACS Publications website at DOI: 10.1021/acs.langmuir.8b01682.

Additional FTIR and XPS data of the brushes (PDF)

■ AUTHOR INFORMATION

Corresponding Author

*E-mail: j.gautrot@qmul.ac.uk.

ORCID

Julien E. Gautrot: 0000-0002-1614-2578

Notes

The authors declare no competing financial interest.

■ ACKNOWLEDGMENTS

We thank Dr Burcu Colak for assistance with some of the thiol-ene coupling experiments. Funding from the Royal Society (RG110425) and the China Scholarship Council (supporting P.T.; grant 201306890005) are acknowledged. S.D.C. thanks QMUL for a studentship.

DOI: 10.1021/acs.langmuir.8b01682
Langmuir XXXX, XXX, XXX−XXX

REFERENCES

(1) Jiang, S.; Cao, Z. Ultralow-fouling, functionalizable, and hydrolyzable zwitterionic materials and their derivatives for biological applications. *Adv. Mater.* **2010**, *22*, 920−932.

(2) Ladd, J.; Zhang, Z.; Chen, S.; Hower, J. C.; Jiang, S. Zwitterionic polymers exhibiting high resistance to nonspecific protein adsorption from human serum and plasma. *Biomacromolecules* **2008**, *9*, 1357−1361.

(3) Yang, W.; Xue, H.; Li, W.; Zhang, J.; Jiang, S. Pursuing "Zero" Protein Adsorption of Poly(carboxybetaine) from Undiluted Blood Serum and Plasma. *Langmuir* **2009**, *25*, 11911−11916.

(4) Rodriguez-Emmenegger, C.; Brynda, E.; Riedel, T.; Houska, M.; Šubr, V.; Alles, A. B.; Hasan, E.; Gautrot, J. E.; Huck, W. T. S. Polymer brushes showing non-fouling in blood plasma challenge the currently accepted design of protein resistant surfaces. *Macromol. Rapid Commun.* **2011**, *32*, 952−957.

(5) Krishnamoorthy, M.; Hakobyan, S.; Ramstedt, M.; Gautrot, J. E. Surface-Initiated Polymer Brushes in the Biomedical Field: Applications in Membrane Science, Biosensing, Cell Culture, Regenerative Medicine and Antibacterial Coatings. *Chem. Rev.* **2014**, *114*, 10976−11026.

(6) Ma, H.; Hyun, J.; Stiller, P.; Chilkoti, A. "Non-Fouling" Oligo(ethylene glycol)- Functionalized Polymer Brushes Synthesized by Surface-Initiated Atom Transfer Radical Polymerization. *Adv. Mater.* **2004**, *16*, 338−341.

(7) Rodriguez Emmenegger, C.; Brynda, E.; Riedel, T.; Sedlakova, Z.; Houska, M.; Alles, A. B. Interaction of blood plasma with antifouling surfaces. *Langmuir* **2009**, *25*, 6328−6333.

(8) de los Santos Pereira, A.; Rodriguez-Emmenegger, C.; Surman, F.; Riedel, T.; Alles, A. B.; Brynda, E. Use of pooled blood plasmas in the assessment of fouling resistance. *RSC Adv.* **2014**, *4*, 2318−2321.

(9) Wu, J.; Lin, W.; Wang, Z.; Chen, S.; Chang, Y. Investigation of the Hydration of Nonfouling Material Poly(sulfobetaine methacrylate) by Low-Field Nuclear Magnetic Resonance. *Langmuir* **2012**, *28*, 7436−7441.

(10) Shao, Q.; He, Y.; White, A. D.; Jiang, S. Difference in hydration between carboxybetaine and sulfobetaine. *J. Phys. Chem. B* **2010**, *114*, 16625−16631.

(11) Gunkel, G.; Weinhart, M.; Becherer, T.; Haag, R.; Huck, W. T. S. Effect of polymer brush architecture on antibiofouling properties. *Biomacromolecules* **2012**, *12*, 4169−4172.

(12) Chen, S.; Li, L.; Zhao, C.; Zheng, J. Surface hydration: principles and applications toward low-fouling/nonfouling biomaterials. *Polymer* **2010**, *51*, 5283−5293.

(13) Trmcic-Cvita, J.; Hasan, E.; Ramstedt, M.; Li, X.; Cooper, M. A.; Abell, C.; Huck, W. T. S.; Gautrot, J. E. Bio-functionalized protein resistant oligo(ethylene glycol)-derived polymer brushes as selective immobilization and sensing platforms. *Biomacromolecules* **2009**, *10*, 2885−2894.

(14) Tugulu, S.; Arnold, A.; Sielaff, I.; Johnsson, K.; Klok, H.-A. Protein-functionalized polymer brushes. *Biomacromolecules* **2005**, *6*, 1602−1607.

(15) Schüwer, N.; Geue, T.; Hinestrosa, J. P.; Klok, H.-A. Neutron reflectivity study on the postpolymerization modification of poly(2-hydroxyethyl methacrylate) brushes. *Macromolecules* **2011**, *44*, 6868−6874.

(16) Barbey, R.; Laporte, V.; Alnabulsi, S.; Klok, H.-A. Postpolymerization Modification of Poly(glycidyl methacrylate) Brushes: An XPS Depth-Profiling Study. *Macromolecules* **2013**, *46*, 6151−6158.

(17) Tan, K. Y.; Ramstedt, M.; Colak, B.; Huck, W. T. S.; Gautrot, J. E. Study of thiol-ene chemistry on polymer brushes and application to surface patterning and protein adsorption. *Polym. Chem.* **2016**, *7*, 979−990.

(18) Pidhatika, B.; Möller, J.; Benetti, E. M.; Konradi, R.; Rakhmatullina, E.; Mühlebach, A.; Zimmermann, R.; Werner, C.; Vogel, V.; Textor, M. The role of the interplay between polymer architecture and bacterial surface properties on the microbial adhesion to polyoxazoline-based ultrathin films. *Biomaterials* **2010**, *31*, 9462−9472.

(19) Pidhatika, B.; Rodenstein, M.; Chen, Y.; Rakhmatullina, E.; Mühlebach, A.; Acikgöz, C.; Textor, M.; Konradi, R. Comparative Stability Studies of Poly(2-methyl-2-oxazoline) and Poly(ethylene glycol) Brush Coatings. *Biointerphases* **2012**, *7*, 1.

(20) Konradi, R.; Acikgoz, C.; Textor, M. Polyoxazolines for Nonfouling Surface Coatings—A Direct Comparison to the Gold Standard PEG. *Macromol. Rapid Commun.* **2012**, *33*, 1663−1676.

(21) Konradi, R.; Pidhatika, B.; Mühlebach, A.; Textor, M. Poly-2-methyl-2-oxazoline: a peptide-like polymer for protein-repellent surfaces. *Langmuir* **2008**, *24*, 613−616.

(22) Kroning, A.; Furchner, A.; Adam, S.; Uhlmann, P.; Hinrichs, K. Probing carbonyl-water hydrogen-bond interactions in thin polyoxazoline brushes. *Biointerphases* **2016**, *11*, 019005.

(23) Knop, K.; Pretzel, D.; Urbanek, A.; Rudolph, T.; Scharf, D. H.; Schallon, A.; Wagner, M.; Schubert, S.; Kiehntopf, M.; Brakhage, A. A.; Schacher, F. H.; Schubert, U. S. Star-shaped drug carriers for doxorubicin with POEGMA and POEtOxMA brush-like shells: a structural, physical, and biological comparison. *Biomacromolecules* **2013**, *14*, 2536−2548.

(24) He, T.; Jańczewski, D.; Jana, S.; Parthiban, A.; Guo, S.; Zhu, X.; Lee, S. S.-C.; Parra-Velandia, F. J.; Teo, S. L.-M.; Vancso, G. J. Efficient and robust coatings using poly(2-methyl-2-oxazoline) and its copolymers for marine and bacterial fouling prevention. *J. Polym. Sci., Part A: Polym. Chem.* **2016**, *54*, 275−283.

(25) Viegas, T. X.; Bentley, M. D.; Harris, J. M.; Fang, Z.; Yoon, K.; Dizman, B.; Weimer, R.; Mero, A.; Pasut, G.; Veronese, F. M. Polyoxazoline: chemistry, properties, and applications in drug delivery. *Bioconjugate Chem.* **2011**, *22*, 976−986.

(26) Rossegger, E.; Schenk, V.; Wiesbrock, F. Design strategies for functionalized poly(2-oxazoline)s and derived materials. *Polymers* **2013**, *5*, 956−1011.

(27) Hoogenboom, R. Poly(2-oxazoline)s: a polymer class with numerous potential applications. *Angew. Chem., Int. Ed.* **2009**, *48*, 7978−7994.

(28) Cortez, M. A.; Grayson, S. M. Thiol−Ene Click Functionalization and Subsequent Polymerization of 2-Oxazoline Monomers. *Macromolecules* **2010**, *43*, 4081−4090.

(29) Kedracki, D.; Chekini, M.; Maroni, P.; Schlaad, H.; Nardin, C. Synthesis and Self-Assembly of a DNA Molecular Brush. *Biomacromolecules* **2014**, *15*, 3375−3382.

(30) Kempe, K.; Weber, C.; Babiuch, K.; Gottschaldt, M.; Hoogenboom, R.; Schubert, U. S. Responsive glyco-poly(2-oxazoline)s: synthesis, cloud point tuning, and lectin binding. *Biomacromolecules* **2011**, *12*, 2591−2600.

(31) Schmitz, M.; Kuhlmann, M.; Reimann, O.; Hackenberger, C. P. R.; Groll, J. Side-Chain Cysteine-Functionalized Poly(2-oxazoline)s for Multiple Peptide Conjugation by Native Chemical Ligation. *Biomacromolecules* **2015**, *16*, 1088−1094.

(32) Schenk, V.; Rossegger, E.; Ebner, C.; Bangerl, F.; Reichmann, K.; Hoffmann, B.; Höpfner, M.; Wiesbrock, F. RGD-functionalization of poly(2-oxazoline)-based networks for enhanced adhesion to cancer cells. *Polymers* **2014**, *6*, 264−279.

(33) Schenk, V.; Ellmaier, L.; Rossegger, E.; Edler, M.; Griesser, T.; Weidinger, G.; Wiesbrock, F. Water-developable poly(2-oxazoline)-based negative photoresists. *Macromol. Rapid Commun.* **2012**, *33*, 396−400.

(34) Dargaville, T. R.; Forster, R.; Farrugia, B. L.; Kempe, K.; Voorhaar, L.; Schubert, U. S.; Hoogenboom, R. Poly(2-oxazoline) hydrogel monoliths via thiol-ene coupling. *Macromol. Rapid Commun.* **2012**, *33*, 1695−1700.

(35) Dargaville, T. R.; Hollier, B. G.; Shokoohmand, A.; Hoogenboom, R. Poly(2-oxazoline) hydrogels as next generation three-dimensional cell supports. *Cell Adhes. Migr.* **2014**, *8*, 88−93.

(36) Farrugia, B. L.; Kempe, K.; Schubert, U. S.; Hoogenboom, R.; Dargaville, T. R. Poly(2-oxazoline) hydrogels for controlled fibroblast attachment. *Biomacromolecules* **2013**, *14*, 2724−2732.

DOI: 10.1021/acs.langmuir.8b01682
Langmuir XXXX, XXX, XXX−XXX

(37) Gress, A.; Völkel, A.; Schlaad, H. Thio-click modification of poly[2-(3-butenyl)-2-oxazoline]. *Macromolecules* **2007**, *40*, 7928−7933.
(38) Weber, C.; Becer, R. C.; Baumgaertel, A.; Hoogenboom, R.; Schubert, U. S. Preparation of Methacrylate End-Functionalized Poly(2-ethyl-2-oxazoline) Macromonomers. *Des. Monomers Polym.* **2009**, *12*, 149−165.
(39) Gieseler, D.; Jordan, R. Poly(2-oxazoline) molecular brushes by grafting through of poly(2-oxazoline)methacrylates with aqueous ATRP. *Polym. Chem.* **2015**, *6*, 4678−4689.
(40) Morgese, G.; Benetti, E. M. Polyoxazoline biointerfaces by surface grafting. *Eur. Polym. J.* **2017**, *88*, 470−485.
(41) Karagoz, B.; Gunes, D.; Bicak, N. Preparation of crosslinked poly(2-bromoethyl methacrylate) microspheres and decoration of their surfaces with functional polymer brushes. *Macromol. Chem. Phys.* **2010**, *211*, 1999−2007.
(42) Jordan, R.; Ulman, A. Surface initiated living cationic polymerization of 2-oxazolines. *J. Am. Chem. Soc.* **1998**, *120*, 243−247.
(43) Zheng, X.; Zhang, C.; Bai, L.; Liu, S.; Tan, L.; Wang, Y. Antifouling property of monothiol-terminated bottle-brush poly(methylacrylic acid)-*graft*-poly(2-methyl-2-oxazoline) copolymer on gold surfaces. *J. Mater. Chem. B* **2015**, *3*, 1921−1930.
(44) Adam, S.; Koenig, M.; Rodenhausen, K. B.; Eichhorn, K.-J.; Oertel, U.; Schubert, M.; Stamm, M.; Uhlmann, P. Quartz crystal microbalance with coupled spectroscopic ellipsometry-study of temperature-responsive polymer brush systems. *Appl. Surf. Sci.* **2017**, *421*, 843−851.
(45) Tauhardt, L.; Frant, M.; Pretzel, D.; Hartlieb, M.; Bücher, C.; Hildebrand, G.; Schröter, B.; Weber, C.; Kempe, K.; Gottschaldt, M.; Liefeith, K.; Schubert, U. S. Amine end-functionalized poly(2-ethyl-2-oxazoline) as promising coating material for antifouling applications. *J. Mater. Chem. B* **2014**, *2*, 4883−4893.
(46) An, J.; Liu, X.; Dedinaite, A.; Korchagina, E.; Winnik, F. M.; Claesson, P. M. Effect of solvent quality and chain density on normal and frictional forces between electrostatically anchored thermoresponsive diblock copolymer layers. *J. Colloid Interface Sci.* **2017**, *487*, 88−96.
(47) Agrawal, M.; Rueda, J. C.; Uhlmann, P.; Müller, M.; Simon, F.; Stamm, M. Facile approach to grafting of poly(2-oxazoline) brushes on macroscopic surfaces and applications thereof. *ACS Appl. Mater. Interfaces* **2012**, *4*, 1357−1364.
(48) Yang, J.; Li, L.; Ma, C.; Ye, X. Degradable polyurethane with poly(2-ethyl-2-oxazoline) brushes for protein resistance. *RSC Adv.* **2016**, *6*, 69930−69938.
(49) Zhang, N.; Pompe, T.; Amin, I.; Luxenhofer, R.; Werner, C.; Jordan, R. Tailored poly(2-oxazoline) polymer brushes to control protein adsorption and cell adhesion. *Macromol. Biosci.* **2012**, *12*, 926−936.
(50) Zhu, H.; Mumtaz, F.; Zhang, C.; Tan, L.; Liu, S.; Zhang, Y.; Pan, C.; Wang, Y. A rapid approach to prepare poly(2-methyl-2-oxazoline)-based antifouling coating by UV irradiation. *Appl. Surf. Sci.* **2017**, *426*, 817−826.
(51) Morgese, G.; Cavalli, E.; Rosenboom, J.-G.; Zenobi-Wong, M.; Benetti, E. M. Cyclic polymer grafts that lubricate and protect damaged cartilage. *Angew. Chem., Int. Ed.* **2018**, *57*, 1621−1626.
(52) Morgese, G.; Trachsel, L.; Romio, M.; Divandari, M.; Ramakrishna, S. N.; Benetti, E. M. Topological polymer chemistry enters surface science: linear versus cyclic polymer brushes. *Angew. Chem., Int. Ed.* **2016**, *55*, 15583−15588.
(53) Danen, E. H. J.; Sonneveld, P.; Brakebusch, C.; Fässler, R.; Sonnenberg, A. The fibronectin-binding integrins $\alpha5\beta1$ and $\alpha v\beta3$ differentially modulate RhoA-GTP loading, organization of cell matrix adhesions, and fibronectin fibrillogenesis. *J. Cell Biol.* **2002**, *159*, 1071−1086.
(54) Dworak, A.; Trzebicka, B.; Kowalczuk, A.; Tsvetanov, C.; Rangelov, S. Polyoxazolines—mechanism of synthesis and solution properties. *Polimery* **2014**, *59*, 88−94.
(55) Brown, A. A.; Khan, N. S.; Steinbock, L.; Huck, W. T. S. Synthesis of oligo(ethylene glycol) methacrylate polymer brushes. *Eur. Polym. J.* **2005**, *41*, 1757−1765.
(56) Li, D.; Sharili, A. S.; Connelly, J.; Gautrot, J. E. Highly stable RNA capture by dense cationic polymer brushes for the design of cytocompatible, serum-stable siRNA delivery vectors. *Biomacromolecules* **2018**, *19*, 606−615.
(57) Barbey, R.; Lavanant, L.; Paripovic, D.; Schüwer, N.; Sugnaux, C.; Tugulu, S.; Klok, H.-A. Polymer brushes via surface-initiated controlled radical polymerization: synthesis, characterization, properties, and applications. *Chem. Rev.* **2009**, *109*, 5437−5527.
(58) Gautrot, J. E.; Trappmann, B.; Oceguera-Yanez, F.; Connelly, J.; He, X.; Watt, F. M.; Huck, W. T. S. Exploiting the superior protein resistance of polymer brushes to control single cell adhesion and polarisation at the micron scale. *Biomaterials* **2010**, *31*, 5030−5041.
(59) Yandi, W.; Mieszkin, S.; Martin-Tanchereau, P.; Callow, M. E.; Callow, J. A.; Tyson, L.; Liedberg, B.; Ederth, T. Hydration and chain entanglement determines the optimum thickness of poly(HEMA-co-PEG10MA) brushes for effective resistance to settlement and adhesion of marine fouling organisms. *ACS Appl. Mater. Interfaces* **2014**, *6*, 11448−11458.
(60) Zhao, C.; Li, L.; Wang, Q.; Yu, Q.; Zheng, J. Effect of film thickness on the antifouling performance of poly(hydroxy-functional methacrylates) grafted surfaces. *Langmuir* **2011**, *27*, 4906−4913.
(61) Liu, Q.; Singh, A.; Lalani, R.; Liu, L. Ultralow fouling polyacrylamide on gold surfaces via surface-initiated atom transfer radical polymerization. *Biomacromolecules* **2012**, *13*, 1086−1092.
(62) Wang, D. K.; Varanasi, S.; Fredericks, P. M.; Hill, D. J. T.; Symons, A. L.; Whittaker, A. K.; Rasoul, F. FT-IR characterization and hydrolysis of PLA-PEG-PLA based copolyester hydrogels with short PLA segments and a cytocompatibility study. *J. Polym. Sci., Part A: Polym. Chem.* **2013**, *51*, 5163−5176.
(63) Nagelsdiek, R.; Mennicken, M.; Maier, B.; Keul, H.; Höcker, H. Synthesis of polymers containing cross-linkable groups by atom transfer radical polymerization: poly(allyl methacrylate) and copolymers of allyl methacrylate and styrene. *Macromolecules* **2004**, *37*, 8923−8932.
(64) Colak, B.; Da Silva, J. C. S.; Soares, T. A.; Gautrot, J. E. Impact of the molecular environment on thiol-ene coupling for biofunctionalization and conjugation. *Bioconjugate Chem.* **2016**, *27*, 2111−2123.
(65) Colak, B.; di Cio, S.; Gautrot, J. E. Biofunctionalised patterned polymer brushes via thiol-ene coupling for the control of cell adhesion and the formation of cell arrays. *Biomacromolecules* **2018**, *19*, 1445.
(66) Hoyle, C. E.; Bowman, C. N. Thiol-ene click chemistry. *Angew. Chem., Int. Ed.* **2010**, *49*, 1540−1573.
(67) Anseth, K. S.; Metters, A. T.; Bryant, S. J.; Martens, P. J.; Elisseeff, J. H.; Bowman, C. N. In situ forming degradable networks and their application in tissue engineering and drug delivery. *J. Controlled Release* **2002**, *78*, 199−209.
(68) McClellan, S. J.; Franses, E. I. Adsorption of bovine serum albumin at solid/aqueous interfaces. *Colloids Surf., A* **2005**, *260*, 265−275.
(69) Gautrot, J. E.; Wang, C.; Liu, X.; Goldie, S. J.; Trappmann, B.; Huck, W. T. S.; Watt, F. M. Mimicking normal tissue architecture and perturbation in cancer with engineered micro-epidermis. *Biomaterials* **2012**, *33*, 5221−5229.
(70) Tan, K. Y.; Lin, H.; Ramstedt, M.; Watt, F. M.; Huck, W. T. S.; Gautrot, J. E.; Gautrot, J. E. Decoupling geometrical and chemical cues directing epidermal stem cell fate on polymer brush-based cell micro-patterns. *Integr. Biol.* **2013**, *5*, 899.
(71) Connelly, J. T.; Gautrot, J. E.; Trappmann, B.; Tan, D. W.-M.; Donati, G.; Huck, W. T. S.; Watt, F. M. Actin and serum response factor transduce physical cues from the microenvironment to regulate epidermal stem cell fate decisions. *Nat. Cell Biol.* **2010**, *12*, 711−718.
(72) McBeath, R.; Pirone, D. M.; Nelson, C. M.; Bhadriraju, K.; Chen, C. S. Cell Shape, Cytoskeletal Tension, and RhoA Regulate Stem Cell Lineage Commitment. *Dev. Cell* **2004**, *6*, 483−495.

DOI: 10.1021/acs.langmuir.8b01682
Langmuir XXXX, XXX, XXX−XXX